Twin Motion Faster Than the Speed of Sound

Eilon Faran and Doron Shilo

Department of Mechanical Engineering, Technion, Haifa 32000, Israel

(Received 31 August 2009; published 14 April 2010)

Twin growth is commonly thought to be bounded by the velocity of shear waves C_T at which the information about this mechanical process travels in the material. Here, we report on experimental evidence of twin growth faster than the material's speed of sound. Driven by an electric field, needle twins in a ferroelectric crystal grew at intersonic speed, with an estimated average velocity close to $\sqrt{2}C_T$. These results strengthen recent theoretical indications of intersonic dislocation motion, and contribute to the understanding of several twin motion-related processes.

DOI: 10.1103/PhysRevLett.104.155501 PACS numbers: 62.20.−x, 77.80.Fm, 81.30.Kf, 81.70.Bt

Common sense implies that the velocity of a propagating material defect that is accompanied by mechanical deformations should be smaller than the velocity at which the information about this defect travels in the material. The latter is the velocity of elastic waves, which depends on the directions of mechanical displacement and wave propagation. Similarly to the theory of relativity, linear elasticity predicts that when a crystal defect such as a dislocation moves at the shear wave speed, its energy, effective mass, and core thickness become infinitely large. However, recent theoretical predictions and experimental observations indicate that several shear-dominated material defects, described in Table I, may propagate at intersonic speeds, i.e., speeds that exceed the material's shear wave velocity.

The most studied shear process in this respect is the propagation of intersonic cracks. Classical fracture mechanics theory predicts that for all crack modes, the energy release rate at the crack tip vanishes if the crack velocity reaches the Rayleigh velocity, C_R, which is the speed at which elastic waves propagate along the crack surfaces. Nevertheless, it can be shown that for mode II cracks, steady state motion is allowed at velocities between the shear and longitudinal wave speed (C_T and C_L, respectively) [1], in particular, around $\sqrt{2}C_T$ [2,3]. Experimental evidences of natural intersonic shear waves first arose from seismographic data of several geological events (see, for example, Refs. [17,18]), in which the estimated rupture velocity approached $\sqrt{2}C_T$ of the Earth's crust.

On a laboratory scale, Rosakis *et al.* [7–9] clearly showed intersonic cracks in a homogeneous brittle polymer, reaching speeds close to $\sqrt{2}C_T$ at steady state. Peterson *et al.* [10] measured crack velocities in stretched rubber that exceeded the shear wave velocity of the material by 10–20%. The existence of intersonic shear cracks is supported by several theoretical works, based both on continuum elastodynamics solutions [4,5] and molecular dynamics [4,6].

From the elasticity point of view, cracks and dislocations are both stress singularities. It is therefore not surprising that theoretical analysis of dislocation motion yields similar results to that of cracks. That is, at C_T, the energy needed to propagate the dislocation diverges, but intersonic steady state motion is allowed under specific conditions and, in particular, at $\sqrt{2}C_T$, which is a stable solution [19]. Using atomistic simulations, Gumbsch *et al.* [11] showed that dislocation velocities may exceed C_T if the dislocations are created at supersonic speeds and sufficient stresses are continuously supplied to preserve these high speeds. Similar results were obtained in Ref. [12] by means of augmented Peierls model. The obtained kinetic relation between the applied shear stress and the dislocation velocity predicts both steady state motion around $\sqrt{2}C_T$ and regions of unstable motion at speeds close to C_R and C_L. Recently, supersonic dislocations in a two-dimensional plasma crystal have been experimentally presented [13].

Dislocation models can be used to describe the structure and motion of planar material defects, such as twin walls [20,21] and martensite-austenite interfaces [22]. Therefore, intersonic propagation may also appear in twinning and martensitic transformations. Using a continuum model for dynamic twinning in crystals, Rosakis [16] predicted that above a critical stress value, the forward growth of a needlelike twin may be intersonic. Recently, it was shown both analytically and by numerical simulation that supersonic motion of steps along a martensite phase boundary is permitted [14,15]. Until now, however, measured velocities of twin and martensite growth have all been subsonic (see, for example, Refs. [23–25]). In Ref. [26], transonic twin growth has been conjectured, but no experimental evidence has been provided.

In this work, we report on intersonic twin growth in ferroelectric $BaTiO_3$ under an electric field. $BaTiO_3$ is considered to be a prototypical ferroelectric crystal, and its structure is similar to that of tetragonal $PbTiO_3$ and lead zirconate titanate (PZT). In these crystals, spontaneous polarization is restricted to lie along one of the $\langle 100 \rangle$ crystallographic directions. Thus, two adjacent domains can have a polarization difference of either 180 or 90 degrees. The former involves no strain change between domains and is the basic mechanism in ferroelectric memory devices [27]. Ninety degree domains, which are actually

TABLE I. Current data on intersonic motion of shear-dominated materials defects.

Intersonic Phenomena	Theoretical predictions and simulations	Experimental observations
Cracks	Yes [1–6]	Yes [7–10]
Dislocations	Yes [11,12]	Yes [13]
Martensitic transformation	Yes [14,15]	N.A.
Twins	Yes [16]	Reported in this Article

twins, are associated with strain change and have a critical role in transducer and actuator applications [28].

The dynamics of individual twins is investigated by means of a unique experimental system that allows for the application of a tunable twinning driving force during a tunable time interval, by means of an electric pulse with amplitude of up to 10 kV and a rise/fall time as low as 0.1 μs. The motion of twin walls is tracked by observing their position before and after the pulse application. This concept has been applied in numerous studies of dislocation dynamics and 180° domain walls (see, for example, Refs. [29,30]) and is based on the evaluation that the inertia of these crystal defects is negligible, and hence, there is a fundamental relationship between their velocity and the driving force for their motion. Indeed, a back-of-the-envelope calculation shows that the distance that a needle twin grows forward after the electric field is turned to zero is less than 1 μm. This estimation is based on the consideration that the forward growth takes place by a collective motion of twin-wall steps. These steps are linear crystallographic defects similar to a dislocation with a Burgers vector of $b \approx \varepsilon_s a$ [31] (where a is the relevant lattice spacing and ε_s is the strain difference between the two domains) and a mass per unit length of $1/2\rho b^2$ [32].

$BaTiO_3$ single crystals cut along the {001} planes to dimensions of $5 \times 5 \times 1$ mm^3 and polished on both surfaces (MTI Crystals Inc.) were tested. The crystals were initially polled to a single domain having a polarization along one of the in-plane ⟨100⟩ directions. Ti electrodes, 20–30 nm thick, were deposited on each of the 5×5 mm^2 surfaces such that the electric field is perpendicular to the initial polarization. An insulating sample holder, having a slot slightly larger than the crystal dimensions, was used to protect the wired crystal without imposing mechanical constraints.

An illustration of the sample's crystallographic direction, the electric field, and the resulting new needle domain is presented in Fig. 1. The interfaces of the new 90 degrees domains are twin walls, and they are associated with a jump in the crystal displacement u along the $[\bar{1}01]$ direction as illustrated in Fig. 1. The forward growth of the needle domain along the [010] direction, which is perpendicular to the displacement vector u, is associated with a shear deformation propagating at the same velocity. The appropriate shear wave speed C_T for these crystallographic directions is given by [33]

$$2\rho C_T^2 = C_{44} + C_{66} + e_{15}^2/\varepsilon_{11} \quad (1)$$

where ρ is the density, and C, e, and ε are the elastic stiffness modulus, piezoelectric and dielectric tensors, respectively. A substitution of $\rho = 6020$ g/cm^3, $C_{44} = 56.2$ GPa, $C_{66} = 127$ GPa, and $e_{15}^2/\varepsilon_{11} = 60.8$ GPa in accordance with [33] provides $C_T = 4500$ m/s.

The new twins are visualized by observing the 5×5 mm^2 sample surfaces under an optical microscope (see illustration in Fig. 1) with a differential interference contrast (DIC), which provides different colors to different inclination angles of the surface. The small angular inclination of the {001} lattice planes on different sides of the twin wall, which appears due to shear strain jump across the wall, is sufficient to form a strong DIC contrast. We verified that this contrast is a result of out-of-plane polarization domains by comparing images taken under DIC and under the cross-polarized transmission mode.

The obtained images exhibit all subprocesses that are involved in twinning, including the nucleation of new twins with a needle shape, the forward growth of needle twins, and the sidewise motion of twin walls. We observed that nucleation occurs at the edge of the crystal and forms new twins with a needle shape as illustrated in Fig. 1. Subsequent pulses of the same amplitude, even with longer duration, do not cause nucleation of new twins. Only the application of a pulse with higher amplitude results in new domains. This behavior can be understood by considering the typical expression for nucleation rate [34], which in our case depends on $\exp(-\delta^2/E^2)$, where E is the electric field and δ is a constant related to the energy barrier for nucleation at room temperature. An evaluation of the energy barrier of a critical nucleus in defect-free $BaTiO_3$ provides $(\delta/E)^2 \sim 10^3$–10^4. This means that nucleation can occur only in defected regions in which the twin-wall energy is

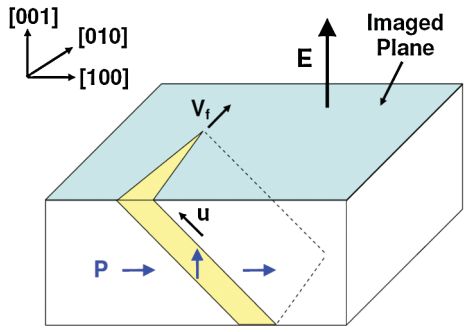

FIG. 1 (color). Schematic view of twin growth under an electric field E applied perpendicular to the initial polarization axis of a $BaTiO_3$ single crystal. The new twin grows at a speed $\boldsymbol{V}_f$ along the [010] direction, while its displacement vector $\boldsymbol{u}$ is along the $[\bar{1}01]$ direction.

significantly smaller than its value in an ideal crystal. Further, if we denote the critical field for nucleation E_N as the field that induces a nucleation rate of one twin per pulse duration (about 1 μs), we see that the ratio $(\delta/E_N)^2$ is about 65 and the exponential term has an order of magnitude of 10^{-28}. Therefore, it is reasonable to assume that for a specific $\delta^{(i)}$ value, which exists in a specific defected region (i) in the crystal, either nucleation occurs immediately after $E > E_N{}^{(i)}$ or no nucleation occurs if $E < E_N{}^{(i)}$.

A typical series of images is presented in Fig. 2 and the electric pulses which were applied between the images are presented in Fig. 3. The amplitude of pulse #1 between images 2(a) and 2(b) was sufficient to nucleate two new twins (marked by **a** and **b**), which grew forward until they crossed the entire crystal width of 5 mm. Pulse #2 between images 2(b) and 2(c) had a higher amplitude, and hence, it induced nucleation of several other twins (marked by letters **c** to **g**), some of which grew forward until they crossed the entire crystal width. During pulse #2, twins **a**, **b**, **c**, **d**, and **e** also grew sideways.

A lower limit for the forward velocity V_f can be calculated by dividing the distance that the twin propagated, i.e., $\Delta x = 5$ mm, by the overall duration $\Delta t = 0.96$ μs for pulse #2, between the two points at which $E = 0$ (see Fig. 3). The actual time which it took for the twin to cross the crystal is equal or shorter than Δt, and hence, $V_f > V_{\min} = \Delta x/\Delta t$. This calculation provides $V_{\min} = 5200$ m/s $\cong 1.16 C_T$.

It has been shown that there is a critical distance, d_C, between the twin tip and the crystal edge; below it, the twin can grow to the opposite edge even under zero driving force [35,36]. The origin for this effect is the attraction of twin-wall steps to the free surface, similarly to the effect of "image force" on dislocations [36]. Experimental results showed that this critical distance is about 0.85–0.9 of the crystal thickness [36] and a theoretical model estimated it to be 0.63 of the crystal thickness [35]. Because of this effect, there is a possibility that the twin reached the critical distance at the end of the pulse and then continued to grow spontaneously. In this case, the actual twin length at the end of the pulse is $\Delta x = 5$ mm $- d_C > 4.1$ mm, and the lower limit for the twin velocity is $V_{\min} = 0.95 C_T$. This scenario is less likely to occur since part of the twins formed during pulse #2, e.g., twins **c**, **d**, and **e**, grew sideways after they crossed the entire crystal. This means that they finished crossing the crystal before the pulse was ended. Theoretical and experimental studies of both cracks and dislocations show that there is a range of forbidden velocity values between C_R and C_T [1,7,12,29]. If this rule holds for twins too, then the result $V_f > 0.95 C_T$ practically means that $V_f > C_T$.

A more realistic evaluation of the electric fields in which the forward growth begins and ends can provide an estimation of the average forward velocity. Since pulse #1 exposed the crystal to $E \geq 13$ kV/cm for a duration of 0.4 μs, we assume that the new twins which appeared after pulse #2 nucleated at a critical field larger than 13 kV/cm. Therefore, we take the time at which $E \geq 13$ kV/cm (marked as t_s in Fig. 3) as the beginning of the forward growth. Estimation of the threshold field, which is required for the forward growth, comes from the condition that the energy released due to the growth should be positive. Assuming a semi-infinite twin lamella with a constant width d such that only the needle tip propagates in a piecewise constant manner, as in [16], the free energy associated with an advancement of the tip by Δy is given by

$$\Delta U = (-EP_s hd + 2\sqrt{2}\gamma_{\mathrm{TW}} h)\Delta y \qquad (2)$$

where P_s is the spontaneous polarization, h is the crystal

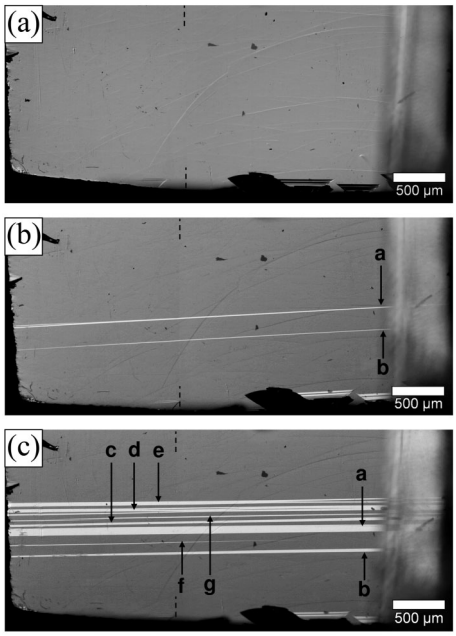

FIG. 2. Optical microscope images showing the twinning process in single crystal $BaTiO_3$ (a) Prior to application of the electric field. (b) After pulse #1; the new twins are marked by letters "a" and "b." (c) After pulse #2; the new twins are marked by letters "c–g".

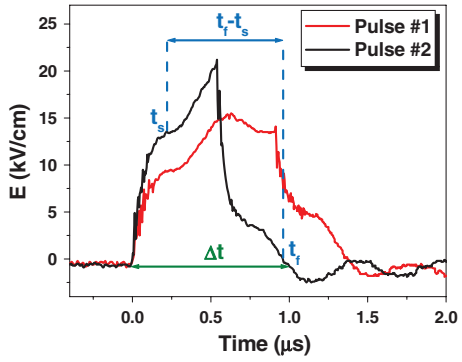

FIG. 3 (color). Electric pulses that induced the twin configurations in Fig. 2. The terms Δt, t_s, and t_f are marked on pulse #2, where Δt is the overall pulse duration and t_s, t_f are the cutoff times denoting the beginning of nucleation and the end of growth, respectively.

thickness, and γ_{TW} is the energy per unit area of the twin wall. The first term in Eq. (2) represents the difference between the energy per unit volume of the polarization P under the external field E, where P and E are perpendicular in the untwined region and parallel within the twin [37,38]. The condition that $\partial \Delta U / \partial \Delta y < 0$ results in

$$E_{\text{thresh}} = 2\sqrt{2}\gamma_{TW}/P_s d. \quad (3)$$

A substitution of $P_s = 0.265$ C/m^2 [39], $\gamma_{TW} = 7$ mJ/m^2 [40] and $d = 4$ μm (according to our obtained images) results in $E_{\text{thresh}} = 0.18$ kV/cm. This value is very close to the threshold field necessary for 90° domain switching as reported in Ref. [30]. We take the time at which E becomes smaller than E_{thresh} (marked as t_f in Fig. 3) as the ending of the forward growth.

An estimation of the average forward velocity as $\bar{V}_f = \Delta x/(t_f - t_s)$, with $\Delta x = 5$ mm, provides $\bar{V}_f = 6670$ m/s $\cong 1.48 C_T$. This value is very close to $\sqrt{2}C_T$, around which theoretical end experimental studies of cracks and dislocations [2,7,11,12,19] show that there is a stable solution.

The possibility of intersonic twin growth may have several important implications. From the application point of view, insight about the dynamics of the twinning process is important since it is responsible for the actuation mechanism in a variety of active materials including ferroelectrics, shape memory alloys (SMA), and ferromagnetic SMA. From a general perspective, the twin's forward growth takes place by a collective motion of twin-wall steps which are linear crystallographic defects similar to dislocations. Therefore, our results strengthen the possibility of intersonic plasticity and intersonic martensitic transformation, which are considered in Table I. Twinning is also the main mechanism of deformation in numerous natural ferroelastic crystals [41], and hence, intersonic twinning may play a role in geological processes, such as attenuation of seismic waves in the Earth's mantle [42].

We thank Mr. Robert Gal and Mr. Yossi Abu for the development of the electric pulser and the experimental system.

[1] K. B. Broberg, Int. J. Fract. **39**, 1 (1989).
[2] L. B. Freund, J. Geophys. Res. **84**, 2199 (1979).
[3] K. B. Broberg, Geophys. J. Int. **119**, 706 (1994).
[4] H. Gao, Y. Huang, and F. F. Abraham, J. Mech. Phys. Solids **49**, 2113 (2001).
[5] E. Dunham, P. Favreau, and J. M. Carlson, Science **299**, 1557 (2003).
[6] F. Abraham and H. Gao, Phys. Rev. Lett. **84**, 3113 (2000).
[7] A. J. Rosakis, O. Samudrala, and D. Coker, Science **284**, 1337 (1999).
[8] K. Xia, A. J. Rosakis, and H. Kanamori, Science **303**, 1859 (2004).
[9] K. Xia, A. J. Rosakis, H. Kanamori, and J. R. Rice, Science **308**, 681 (2005).
[10] P. J. Petersan, R. D. Deegan, M. Marder, and H. L. Swinney, Phys. Rev. Lett. **93**, 015504 (2004).
[11] P. Gumbsch and H. Gao, Science **283**, 965 (1999).
[12] P. Rosakis, Phys. Rev. Lett. **86**, 95 (2001).
[13] V. Nosenko, S. Zhdanov, and G. Morfill, Phys. Rev. Lett. **99**, 025002 (2007).
[14] Y. Zhen and A. Vainchtein, J. Mech. Phys. Solids **56**, 496 (2008).
[15] Y. Zhen and A. Vainchtein, J. Mech. Phys. Solids **56**, 521 (2008).
[16] P. Rosakis and H. Tsai, Int. J. Solids Struct. **32**, 2711 (1995).
[17] M. Bouchon and M. Vallee, Science **301**, 824 (2003).
[18] M. Bouchon, Geophys. Res. Lett. **28**, 2723 (2001).
[19] J. P. Hirth and J. Lothe, *Theory of Dislocations* (Wiley, New York, 1982), 2nd ed., p. 204.
[20] H. Tsai and P. Rosakis, J. Mech. Phys. Solids **49**, 289 (2001).
[21] V. S. Boyko, R. I. Garber, and A. M. Kossevich, *Reversible Crystal Plasticity* (American Institute of Physics, New York, 1994).
[22] M. Grujicic, G. B. Olson, and W. S. Owen, Metall. Mater. Trans. A **16**, 1713 (1985).
[23] D. F. Williams and C. N. Reid, Acta Metall. **19**, 931 (1971).
[24] R. F. Bunshah and R. F. Mehl, J. Met. **5**, 1251 (1953).
[25] V. M. Finkel', A. M. Savel'ev, A. P. Korolev, and V. A. Fedorov, Phys. Met. Metallogr. **46**, 121 (1978).
[26] V. M. Finkel', I. N. Voronov, A. M. Savel'ev, A. I. Yeliscyenko, and V. A. Fedorov, Phys. Met. Metallogr. **29**, 131 (1970).
[27] J. F. Scott, *Ferroelectric Memories* (Springer, New York, 2000), 1st ed.
[28] K. Bhattacharya and G. Ravichandran, Acta Mater. **51**, 5941 (2003).
[29] W. G. Johnston and J. J. Gilman, J. Appl. Phys. **30**, 129 (1959).
[30] E. A. Little, Phys. Rev. **98**, 978 (1955).
[31] P. Mullner and G. Kostorz, Mater. Sci. Forum **583**, 43 (2008).
[32] E. Nadgornyi, Prog. Mater. Sci. **31**, 1 (1988).
[33] Z. Li, S. K. Chan, M. H. Grimsditch, and E. S. Zouboulis, J. Appl. Phys. **70**, 7327 (1991).
[34] D. A. Porter and K. E. Easterling, *Phase Transformations in Metals and Alloys* (Van Nostrand Reinhold Co., USA, 1981), 1st ed.
[35] V. S. Boiko, L. A. Pastur, and E. P. Fel'dman, Sov. Phys. Solid State **8**, 2384 (1967).
[36] V. S. Boiko, R. I. Garber, and L. F. Krivenko, Sov. Phys. Solid State **9**, 332 (1967).
[37] Q. Jiang, J. Elast. **34**, 1 (1994).
[38] D. Shilo, E. Burcsu, G. Ravichandran, and K. Bhattacharya, Int. J. Solids Struct. **44**, 2053 (2007).
[39] W. J. Mertz, Phys. Rev. **95**, 690 (1954).
[40] J. Hlinka, Ferroelectrics **349**, 49 (2007).
[41] E. K. H. Salje, *Phase Transitions in Ferroelastic and Coelastic Crystals* (Cambridge University Press, Cambridge, 1993).
[42] R. J. Harrison and S. A. T. Redfern, Phys. Earth Planet. Inter. **134**, 253 (2002).